JOURNAL
OF THE AMERICAN CHEMICAL SOCIETY

VOLUME 104, NUMBER 9 MAY 5, 1982

Fragmentation Mechanism and Energetics of Some Alkyl Halide Ions

H. M. Rosenstock, R. Buff,* M. A. A. Ferreira, S. G. Lias, A. C. Parr, R. L. Stockbauer, and J. L. Holmes

Contribution from the National Bureau of Standards, Washington, DC 20234, and Department of Chemistry, University of Ottawa, Ottawa, Ontario, K1N 9B4, Canada.

Received August 17, 1981

Abstract: Halogen loss from iodoethane, 1-bromopropane, 2-bromopropane, 1-iodopropane, and 2-iodopropane has been studied by means of electron–ion coincidence techniques and by observation of metastable transition. Analysis of the breakdown curves and the study of residence times gave the zero-kelvin thresholds for halogen loss and indicated the size of the kinetic shift. The fragmentation onset for iodoethane was located in a Franck–Condon gap. The zero-kelvin thresholds for the propyl halides were found to lie at or just above the upper spin–orbit level of the parent ion. All of the propyl halides exhibited a unimolecular metastable transition. At fragmentation onset the 2-halopropane ions have negligible fragment kinetic energy while the 1-halopropane produce secondary propyl ions with 100–200 meV of kinetic energy. It was established that a potential barrier must be surmounted in this fragmentation–isomerization process and analysis suggests a dynamic mechanism other than conventional QET, for example, weak couplings of vibrational modes. Analysis of the 2-halopropane fragmentation thresholds leads to an accurate, absolute value for the proton affinity of propylene, 751.4 ± 2.9 kJ/mol at room temperature. This value reconciles some differences inherent in the proton affinity scale based on various relative measurements.

The determination of the heats of formation of the lower alkyl ions is of considerable interest inasmuch as accurate values provide absolute reference points for the gas phase proton affinity scale.[1] Further, the heats of formation can be combined with adiabatic ionization potentials of the radicals to give heats of formation of the neutral radicals. These can be critically compared with the radical heats of formation as determined by chemical kinetics techniques[2,3] and (hopefully) provide an independent verification leading to greater confidence in the body of experimental technique.

Recently the zero-kelvin heat of formation of the ethyl ion was determined by a photoelectron–photoion coincidence study of the fragmentation of ethyl iodide.[4] Also, the heat of formation of this ion[5] as well as that of the secondary[4,6] propyl ion has been determined by a study of the photoion fragmentation threshold in a number of ethyl and propyl halides. Finally, it has been established that at threshold the etthyl iodide ion produces fragments with negligible kinetic energy.[7] The values of the ion heats of formation thus far obtained appear reproducible and self-consistent. However, when combined with the radical ionization potentials recently determined by photoelectron spectroscopy,[8] they yield values for the heats of formation of the radicals which are in some disagreement with the values obtained by various techniques of chemical kinetics. It has been suggested that the discrepancy arises from the fact that the radical ionization potentials are not the adiabatic values.[5]

We have redetermined these ion heats of formation by using photoelectron–photoion coincidence techniques and have obtained some information on fragmentation rates and fragmentation kinetic energy distributions by analysis of the peak shapes of corresponding unimolecular metastable transitions. The molecules iodoethane, 1-iodopropane, 2-iodopropane, 1-bromopropane, and 2-bromopropane were studied. With the coincidence technique employed here it was possible to model the breakdown curves and locate the zero-kelvin fragmentation thresholds as well as to search for kinetic shift effects using the variable residence time capability of the apparatus. Thus we could test the assumption made in previous photoionization studies that an extrapolation of the linear portion of the fragment ion yield curve gives an effective room-temperature fragmentation threshold.[5] This assumption is somewhat difficult to justify in a clear manner. It requires at the very least that the Franck–Condon factors for ionization–excitation

---

*To whom correspondence should be addressed at the Department of Physics, University of Alabama, University, Alabama 35486. Intergovernmental Personnel Act Appointee, 1980–1981. M.A.A.F., Guest worker, Faculty of Science, University of Lisbon, Lisbon, Portugal. H.M.R., R.B., S.G.L., A.C.P., and R.L.S., National Bureau of Standards. J.L.H., University of Ottawa.

(1) See, for example, D. H. Aue and M. T. Bowers in M. T. Bowers, Ed. "Gas Phase Ion Chemistry", Academic Press, New York. 1979, Chapter 9.

(2) See, for example, W. Tsang in A. Lifschitz, Ed., "Shock Tubes in Technology", Marcel Dekker, New York, 1981.

(3) W. Tsang, *Int. J. Chem. Kinet.*, **10**, 821 (1978).

(4) T. Baer, *J. Am. Chem. Soc.*, **102**, 2482 (1980).

(5) J. C. Traeger and R. G. McLoughlin, *J. Am. Chem. Soc.*, **103**, 3647 (1981).

(6) J. C. Traeger, *Int. J. Mass Spectrom. Ion Phys.*, **32**, 309 (1980).

(7) T. Baer, U. Büchler, and C. E. Klots, *J. Chim. Phys.*, **77**, 739 (1981).

(8) F. A. Houle and J. L. Beauchamp, *J. Am. Chem. Soc.*, **101**. 4067 (1979).

0002-7863/82/1504-2337$01.25/0

of the parent molecule be constant in the neighborhood of the fragmentation threshold.

In addition to their thermochemical interest, the fragmentation processes in question—loss of a halogen atom, possibly accompanied by isomerization—pose interesting questions about the behavior of the various spin–orbit states of the ions. Accordingly, the threshold photoelectron spectra of all five compounds were determined as well.

Experimental Section

Breakdown curves for the five alkyl halides were obtained by using the photoelectron–photoion coincidence apparatus[9] and methodology previously described.[10,11] Briefly, the sample is photoionized by a photon beam which is dispersed by a 1-m Seya-Namioka monochromator. The photoelectrons formed in the source region are accelerated toward the electron analyzer–detector system by a weak (0.8 V/cm) static electrostatic field. The electrons are energy selected by passage through a steradiancy analyzer followed by a 127° electrostatic sector analyzer. This array allows passage principally of electrons initially formed with near-zero kinetic energy. Some higher energy electrons with initial velocities directed toward the electron analyzer system will also be detected. The electron energy sampling function thus is strongly peaked, is slightly broadened due to finite electron and photon monochromator resolution, and is tailed toward higher acceptance energy as a result of detection of some of these "hot electrons". The form of the sampling function can be determined from measurement of the relative collection efficiency of photoelectrons produced at and above the krypton $^2P_{1/2}$ ionization threshold.[9] This sampling function was redetermined in the course of the present experiments and was identical with that previously determined and shown in ref 9. It has a width of 26-meV fwhm. Following detection of an electron, an ion ejection pulse is applied to the source region and the ions are ejected, passed through an acceleration and drift region, and finally detected on an ion multiplier. For a study of kinetic shift effects, the time of application of the ejection pulse can be delayed for a number of microseconds, thus increasing the time available for ion fragmentation (and rearrangement) in the source region. The relative parent and fragment ion abundances can thus be measured at different photon energies and the data assembled to give the breakdown curve at one or another ion source residence time.

The metastable transitions were studied in the first field-free region of a Kratos-AEI MS902S double-focusing mass spectrometer.[12] Precautions were taken to eliminate interference from collision-induced dissociation processes. These included careful study of the effect of pressure on the abundances of the metastable transitions as well as on their peak shapes. The analysis of the peak shapes to yield total fragmentation kinetic energy distributions was carried out as previously described.[12-15] In addition, with available beam trajectory calculations it was possible to determine the range of unimolecular fragmentation rates which would yield observable metastable transitions[16] (see below).

The relative abundances of the molecular ions and the first field-free region metastable peaks for halogen atom loss were estimated as follows. The metastable peak intensity was measured from the peak height (at low-energy resolution where the entire ion beam is collected[16]) of the transmitted m/z 43 ions at an acceleration voltage of 7100 V. The molecular ion peak intensities were then measured without changing the source conditions; i.e., only the electric sector and the magnetic field were changed. No correction was made for possible differences in detection sensitivity due to the different impact velocities of the parent and metastable ions on the Daly detector emitter. This omission probably leads to a slight underestimate of the metastable to parent ion ratio. The ratio of metastable to parent ion was measured at various ion source pressures, ranging from 5×10^{-8} to 8×10^{-7} torr, in order to assess and eliminate any possible contributions from collision induced dissociations.

Table I. Threshold Values of Ethyl Iodide Ion Fragmentation

crossover energy, eV	threshold, eV	temp, K	method	ref
10.48 ± 0.01	10.52 ± 0.01	0	coincidence	this work
10.43	10.49	0	coincidence	4
. . .	10.44 ± 0.01	298	photoionization	5
. . .	>10.42 ± 0.05	298	photoionization	18

Table II. Auxiliary Thermochemistry

molecule	$\Delta H_f{}^\circ{}_0$, kJ/mol	$\Delta H_f{}^\circ{}_{298}$, kJ/mol	$H_{298} - H_0$, kJ/mol	ref	comments
C(graphite)	0	0	1.05	19	
H_2	0	0	8.47	19	
Br_2	0	0	24.51	19	
Br	117.94 ± 0.3	111.88	6.20	19	
I_2	0	0	13.20	19	
I	107.25 ± 0.04	106.85	6.20	19	
C_2H_5I	7.5 ± 2	−8.37 ± 2	13.85	17	
1-C_3H_7Br	−56.2	−84.5 ± 0.5	16.78	44	$H_{298} - H_0$ and $\Delta H_f{}^\circ{}_0$ calculated in this work
2-C_3H_7Br	−70.4 ± 1	−98.3 ± 0.9	17.21	44	
1-C_3H_7I	−10.2 ± 2	−32.5 ± 1.7	17.07	44	
2-C_3H_7I	−20.1 ± 2	−41.6 ± 1.7	17.15	44	
C_2H_5	. . .	. . .	12.38	5	
$C_2H_5{}^{+a}$	. . .	. . .	11.46	5	
2-C_3H_7	. . .	. . .	16.03	5	
2-$C_3H_7{}^{+a}$	. . .	. . .	15.44	5	

[a] Using the stationary electron convention.

Table III. Ethyl Ion Heat of Formation

parent molecule	$\Delta H_f{}^\circ{}_0$, kJ/mol	$\Delta H_f{}^\circ{}_{298}$,[a] kJ/mol	method	ref
C_2H_5I	915.3 ± 2	903.5 ± 2	coincidence	this work
C_2H_5I	913.0 ± 4	900.8 ± 4	coincidence	4
C_2H_6 C_2H_5Cl C_2H_5Br C_2H_5I	. . .	903.7 ± 2	photoionization	5
		900.0 ± 7	ion–molecule equilibrium	56

[a] Using the stationary electron convention.[55]

Results

The breakdown curves for the ethyl iodide, 1-iodopropane, 2-iodopropane, 1-bromopropane, and 2-bromopropane are shown in Figures 1–5. In Figure 6 the total fragment kinetic energy distribution is shown for the metastable transition corresponding to loss of an iodine atom from 1-iodopropane parent ion. The form of this distribution arises from the almost pure Gaussian peak shape of the experimentally observed metastable transition. The metastable peaks for the other propyl halide ions were also of Gaussian type but with different kinetic energy release distributions (see below).

Ethyl Iodide. The breakdown curves obtained at 0.7- and 5.7-μs nominal ion source residence time indicate that there is no detectable time shift, see Figure 1. Hence one can assume a step function behavior for the fragment ion yield as the excitation energy is increased. In such a case the form of the breakdown curve should be describable by convolution of the step function with the apparatus function and the thermal energy content of the molecule.[10] The vibrational energy distribution of the molecule at room temperature was obtained from vibrational frequencies tabulated by Kudchadker.[17] Further, it was assumed that all external rotational energy was available for fragmentation. The resulting calculated breakdown curve is in very good agreement

---

(9) R. L. Stockbauer, *Int. J. Mass Spectrom. Ion Phys.*, **25**, 89 (1977).

(10) R. L. Stockbauer and H. M. Rosenstock, *Int. J. Mass Spectrom. Ion Phys.*, **27**, 185 (1978).

(11) H. M. Rosenstock, A. L. Stockbauer, and A. C. Parr, *J. Chem. Phys.*, **71**, 3708 (1979).

(12) J. L. Holmes, A. D. Osborne, and G. M. Weese, *Int. J. Mass Spectrom. Ion Phys.*, 19, 207 (1976).

(13) J. L. Holmes and A. D. Osborne, *Int. J. Mass Spectrom. Ion Phys.*, **23**, 189 (1977).

(14) J. L. Holmes and A. D. Osborne, *Int. J. Mass Spectrom. Ion Phys.*, **27**, 271 (1978).

(15) J. L. Holmes, K. Cartledge, and A. D. Osborne, *Int. J. Mass Spectrom. Ion Phys.*, **29**, 171 (1979).

(16) J. L. Holmes and J. K. Terlouw, *Org. Mass Spectrom.*, **15**, 383 (1980).

(17) S. A. Kudchadker and A. P. Kudchadker, *J. Phys. Chem. Ref. Data*, **8**, 519 (1979).

(18) M. E. Akopyan, Y. L. Sergeev, and F. I. Vilesov, *Khim. Vys. Energ.*, **4**, 213 (1970).

(19) D. R. Stull and H. Prophet, *Natl. Stand. Ref. Data Ser.* (*U.S., Natl. Bur. Stand.*), **NSRDS-NBS 37** (1970).

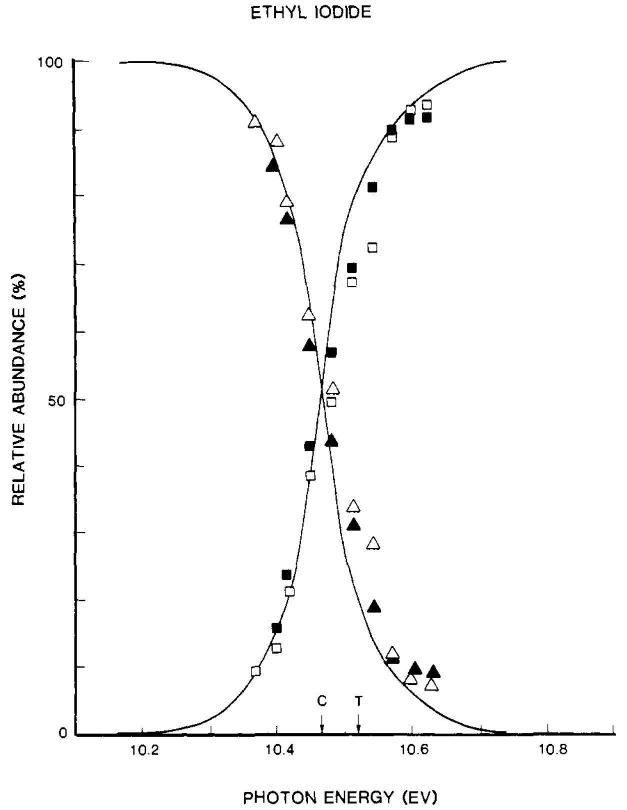

Figure 1. Breakdown curve for $C_2H_5I^+$ fragmentation at 0.7 μsec (△, □) and 5.7 μs (▲, ■) nominal ion source residence times. The arrows labeled *C* and *T* indicate the photon energy at the crossover (50% fragmentation) and the energy of the zero-kelvin threshold, respectively.

with experiment. This leads to a fragmentation threshold at absolute zero of 10.52 ± 0.01 eV, compared to the crossover energy of 10.48 ± 0.01 eV at which 50% fragmentation is observed. The results are compared with earlier threshold measurements in Table I. The fragmentation threshold value may then be combined with appropriate thermochemical data, see Table II, to give the zero-kelvin heat of formation of the ethyl ion. The results are in very good agreement with earlier work, as shown in Table III. However, although the zero-kelvin threshold value arrived at in the earlier coincidence study[4] is in rather good agreement with our present results, the experimentally determined crossover energy is significantly lower than observed in the present work. It is to be noted that no correction for the apparatus function was discussed or employed in the earlier work.[4]

As indicated above, extrapolation of the linear portion of a fragment photoionization yield curve has been stated to give an intercept which is effectively a room-temperature threshold. That is to say, it gives a value equal to the zero-kelvin threshold minus the room-temperature average internal thermal energy of the fragmenting ion.[5,20] The apparent validity of this procedure for ethyl iodide ion implies that as the photon energy is swept over the fragmentation threshold there is a linear increase in the population of fragmenting ion states, suggesting in turn an essentially constant value for the parent ion Franck–Condon factors for direct ionization. However, examination of the 58.4-nm photoelectron spectrum[21] and the related threshold photoelectron spectrum, see Figure 7, shows that the threshold lies in a Franck–Condon gap, between the upper spin-orbit component of the ion ground state and the next excited electronic state. Thus near threshold the fragmenting ion states are being produced exclusively by autoionizing action. It would be of considerable interest to study the shape of the photoion fragmentation yield curve out to energies above the onset of the higher electronic state, where direct ionization will occur.

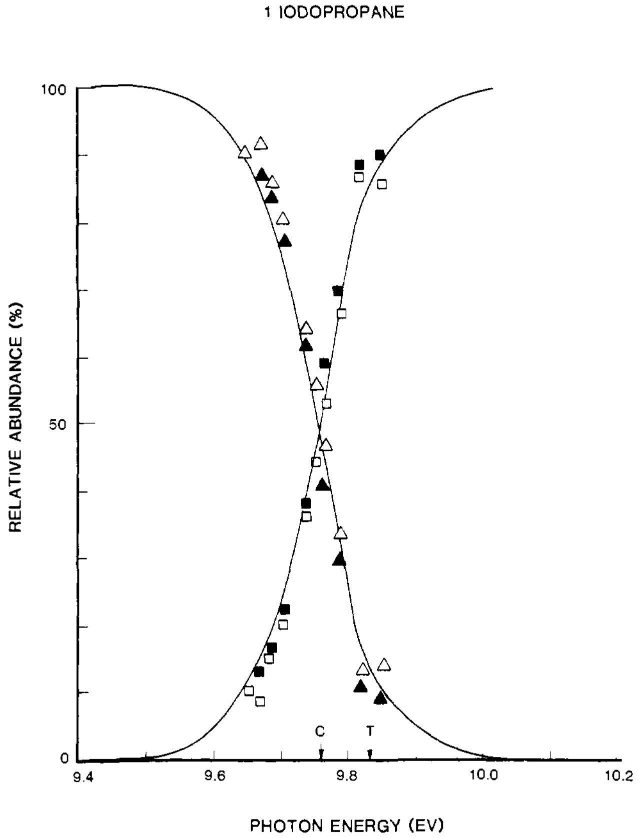

Figure 2. Breakdown curve for 1-$C_3H_7I^+$ fragmentation at 0.7 μs (△, □) and 5.7 μs (▲, ■) nominal ion source residence times. The arrows labeled *C* and *T* indicate the photon energy at the crossover (50% fragmentation) and the energy of the zero-kelvin threshold, respectively.

Table IV. Metastable Transitions of Propyl Halide Parent Ions

Parent Ion	abundance relative to parent	total kinetic energy, meV		
		av	98%	99%
1-$C_3H_7I^+$	$(1.5 \pm 0.1) \times 10^{-3}$	33 ± 1	86 ± 2	100 ± 2
2-$C_3H_7I^+$	$(1.1 \pm 0.1) \times 10^{-4}$	~1.9		~6
1-$C_3H_7Br^+$	$(4.0 \pm 0.1) \times 10^{-3}$	37 ± 2	105 ± 8	120 ± 12
2-$C_3H_7Br^+$	$(1.5 \pm 0.1) \times 10^{-4}$	~0.5		~1.5

2-Iodopropane and 2-Bromopropane. The breakdown curves for 2-iodopropane and 2-bromopropane are shown in Figures 3 and 5. It is seen that, as the nominal ion source residence time is increased from 0.7 to 5.7 μs, there is a slight shift (reproducible in a number of experiments) in both breakdown curves, amounting to about 0.01–0.03 eV. This indicates that near threshold the ions have a lifetime in the microsecond range. In addition, studies with the double-focusing mass spectrometer revealed the presence of unimolecular metastable transitions in both molecule ions, suggesting even longer lifetimes. The results are summarized in Table IV. The significance of the lifetimes will be discussed in a later section.

The shift in the breakdown curves was so small that it was decided to model them by convoluting a step function threshold with the appropriate internal thermal energy distributions, including external rotations. The vibrational frequencies for 2-iodopropane were taken from the literature[22a] with three missing frequencies (246, 253, 262 cm^{-1}) taken from the solid phase.[22b] A complete set of frequencies for 2-bromopropane was available in the literature.[23] The calculated breakdown curves are also shown in Figures 3 and 5, placed on the energy scale to best fit

---

(20) W. A. Chupka, *J. Chem. Phys.*, **54**, 1936 (1971).

(21) R. A. A. Boschi and D. R. Salahub, *Can. J. Chem.*, **52**, 1217 (1974).

(22) (a) N. Sheppard, *Trans. Faraday Soc.*, **46**, 533 (1950). (b) J. R. Durig, C. M. Player, Jr., Y. S. Li, J. Bragin, and C. W. Hawley, *J. Chem. Phys.*, **57**, 4544 (1972).

(23) R. G. Snyder, *J. Mol. Spectrosc.*, **28**, 273 (1968).

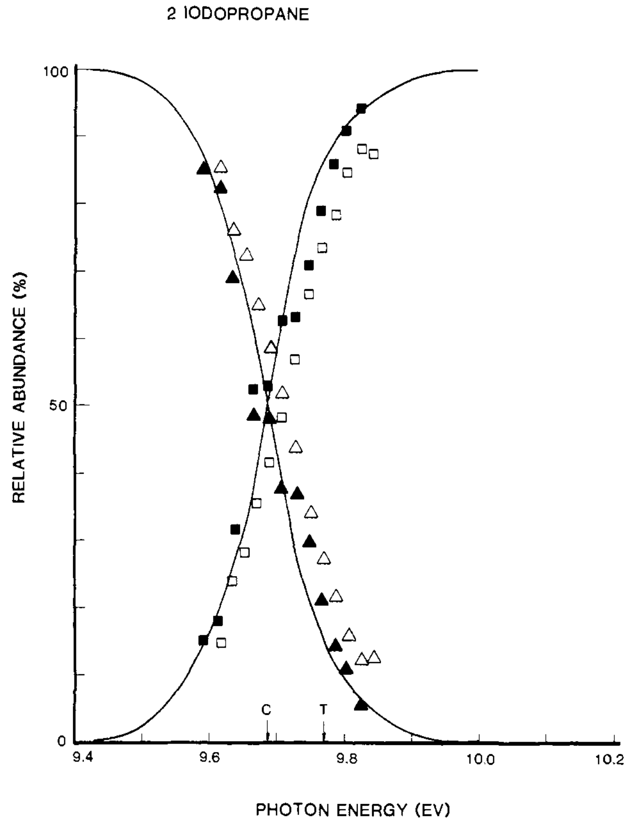

Figure 3. Breakdown curve for 2-$C_3H_7I^+$ fragmentation at 0.7 μs (△, □) and 5.7 μs (▲, ■) nominal ion source residence times. The arrows labeled *C* and *T* indicate the photon energy at the crossover (50% fragmentation) and the energy of the zero-kelvin threshold, respectively.

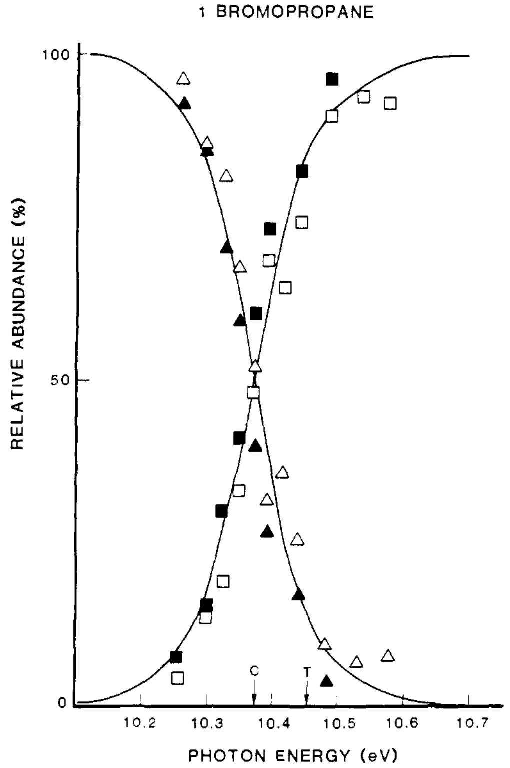

Figure 4. Breakdown curve for 1-$C_3H_7Br^+$ fragmentation at 0.7 μs (△, □) and 5.7 μs (▲, ■) nominal ion source residence times. The arrows labeled *C* and *T* indicate the photon energy at the crossover (50% fragmentation) and the energy of the zero-kelvin threshold, respectively.

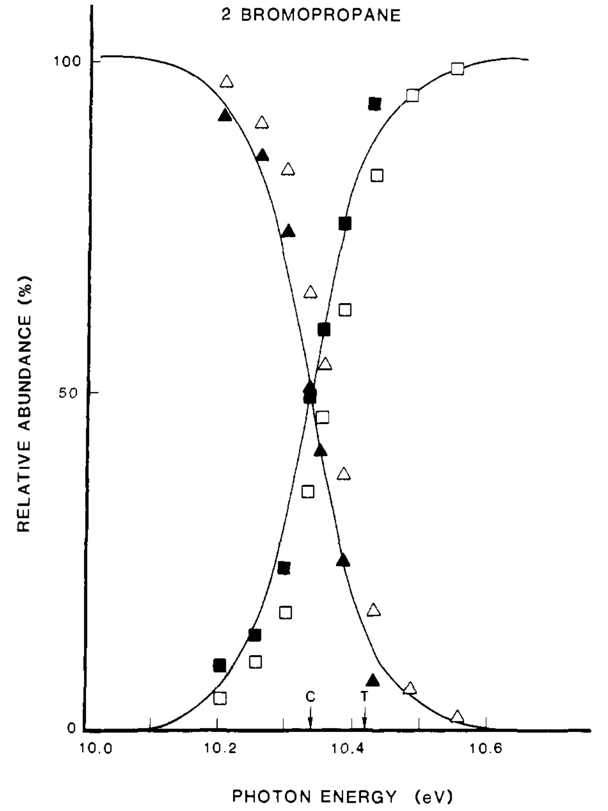

Figure 5. Breakdown curve for 2-$C_3H_7Br^+$ fragmentation at 0.7 μs (△, □) and 5.7 μs (▲, ■) nominal ion source residence times. The arrows labeled *C* and *T* indicate the photon energy at the crossover (50% fragmentation) and the energy of the zero-kelvin threshold, respectively.

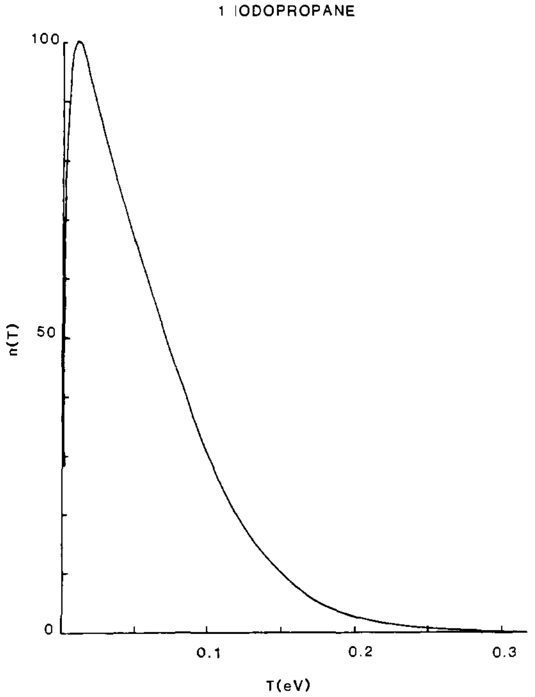

Figure 6. Kinetic energy distribution of the metastable transition for loss of iodine atom by the 1-iodopropane ion.

the set of long-residence time data. It is seen that the curves fit the data reasonably well in both cases. The crossover energies (*C*) and deduced fragmentation thresholds (*T*) are indicated with arrows, and, as discussed in our earlier work,[10,11] the fragmentation threshold lies at higher energies than the crossover.

The narrow Gaussian peak shapes of the unimolecular metastable transitions for both molecules indicate that the loss of a halogen atom is accompanied by very little kinetic energy release, less than 0.01 eV (see Table IV). With the assumption that there is no additional unobservable excess energy at the fragmentation

Table V. Energetics of $C_3H_7^+$ Ions

parent molecule	0 K threshold, eV	kinetic energy correction,[a] eV	$\Delta H_f{}^\circ{}_0$, kJ/mol	$\Delta H_f{}^\circ{}_{298}$, kJ/mol	method	ref
2-C_3H_7Br	10.42 ± 0.01	0.0015	817.9 ± 2	799.5 ± 2	coincidence	this work
2-C_3H_7I	9.77 ± 0.02	0.006	816.4 ± 4	798.2 ± 4	coincidence	this work
2-C_3H_7I		. . .	817.6 ± 2	798.3 ± 2	photoionization	4
2-C_3H_7Cl				802.5 ± 2	photoionization	5
2-C_3H_7Br						
2-C_3H_7I						
C_3H_8				805.4	photoionization, recalculated by Traeger[5]	29
1-C_3H_7Br	10.55 ± 0.01	>0.12	<832 ± 5	<815 ± 5	coincidence	this work
1-C_3H_7I	9.84 ± 0.01	>0.10	<822 ± 5	<805 ± 5	coincidence	this work

[a] See text for discussion of this correction. [b] Using the stationary electron convention.[55]

Table VI. Comparison of Radical Thermochemistry

species	IP, eV	ref	$\Delta H_f{}^\circ{}_0$, kJ/mol	$\Delta H_f{}^\circ{}_0$(radical)[a] kinetics, kJ/mol	ref
$C_2H_5^+$			915.3 ± 2		
C_2H_5	8.39 ± 0.02	8	105.8 ± 3	128–132	3
				122	30
i-$C_3H_7^+$			816.2 ± 4		
i-C_3H_7	7.36 ± 0.02	8	106.0 ± 5	98–105	3
				90	30

[a] Derived from $\Delta H_f{}^\circ{}_{298}$ values corrected to absolute zero with the thermochemical quantities given in Table II.

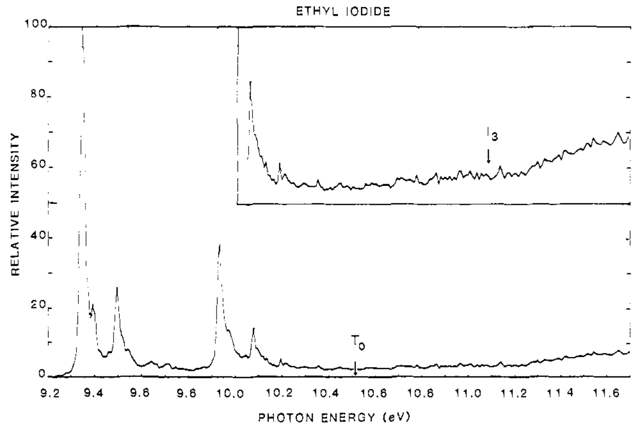

Figure 7. Threshold photoelectron spectrum of ethyl iodide. The arrows labeled T_0 and I_3 indicate the energies of the zero-kelvin threshold and the onset of the first σ electronic state (taken from ref 21), respectively. The inset shows the last portion of this spectrum with an expanded vertical scale.

threshold (such as rotation of the $C_3H_7^+$ ion brought about by recoil against the departing halogen atom) the zero-kelvin fragmentation thresholds can be combined with auxiliary thermochemical data to give the heat of formation of the $C_3H_7^+$ ion, presumed to have the 2-propyl structure. The results are summarized and compared in Table V. They are but slightly different from those of previous workers.

1-Iodopropane and 1-Bromopropane. The breakdown curves for 1-iodopropane and 1-bromopropane are shown in Figures 2 and 4, along with the curves calculated assuming a step function threshold. Molecular frequencies were taken from the compilation of Shimanouchi et al.[24] The experimental data for these two ions show a very slight but systematic displacement, again suggesting a very small dependence on residence time. Both ions, however, give observable unimolecular metastable transitions in the mass spectrometer.

In contrast to the 2-iodo- and 2-bromopropane, the metastable transitions of this pair of ions indicate that the fragmentations are accompanied by significant kinetic energy release. The peak shapes of the transition are also Gaussian in form, but broader. In order to extract thermochemical information from the threshold values determined here, it is necessary to somehow correct for this kinetic energy distribution. This problem has been discussed in detail by Beynon et al.[25-27] and by Franklin,[28] but no satisfactory methodology has emerged. We assume in the present case that the metastable transitions arise from a group of ions with a narrow range of excitation energies and that the observed kinetic energy distributions arise from the various ways of partitioning a well-defined amount of excess energy among the degrees of freedom of the products. This model tacitly assumes that the excess energy requirement arises from a potential barrier which must be overcome in fragmentation. It is in accord with the observation that the parent–daughter transition of the breakdown curves show no marked broadening due to slow dependence of the fragmentation rate on excitation energy. Accordingly, the threshold value should be correct by using the maximum observed kinetic energy. Now the Gaussian peak shape and resulting Boltzmann-like energy distribution has no maximum value; it extends to infinity. More realistically, one should state that the metastable peak shape can be represented by a Gaussian function over that translational energy range where the peak lies above the apparatus noise level. In the present experiments this amounts to about 98–99% of the total of the Gaussian distribution. With this criterion, the kinetic energy of the fragmentation is 86–100 meV for 1-iodopropane and 110–120 meV for 1-bromopropane. The resulting thermochemistry is given in Table V. It is seen that with this correction the $C_3H_7^+$ species formed from the primary propyl compounds has very nearly the same heat of formation as the 2-$C_3H_7^+$ ion, implying that the fragmentation is accompanied by a rearrangement and making plausible the existence of a potential barrier. If we assume that the zero-kelvin thresholds lie at the onset of the upper spin–orbit doublet, the agreement is even closer especially for the 1-bromopropane, see Figure 11 and discussion below. Other evidence for existence of this barrier is presented in a later section.

The approach we have taken here certainly has some weaknesses. The 98 or 99% criterion is somewhat arbitrary and gives a rather imprecise estimate of the maximum energy; but this could be remedied in the future by developing statistical criteria for estimating the maximum peak width of a noisy signal. It is an unfortunate fact that although the half width of a Gaussian peak can be readily determined with good precision, it is not really suitable for making a meaningful energy correction. This is so because the observed metastable kinetic energy distribution is a composite sample representing a distribution of rates and excitation

---

(24) T. Shimanouchi, H. Matsuura, Y. Oyawa, and I. Harada, *J. Phys. Chem. Ref. Data*, 9, 1149 (1980).

(25) E. G. Jones, J. H. Beynon, and R. G. Cooks, *J. Chem. Phys.*, **57**, 2652 (1972).

(26) R. K. Boyd and J. H. Beynon, *Int. J. Mass Spectrom. Ion Phys.*, **23**, 163 (1977).

(27) J. H. Beynon and J. R. Eilbert in M. T. Bowers, Ed., "Gas Phase Ion Chemistry", Vol. II, Academic Press, New York, 1979.

(28) J. L. Franklin in M. T. Bowers, Ed., "Gas Phase Ion Chemistry", Vol. I, Academic Press, New York, 1979.

(29) W. A. Chupka and J. Berkowitz, *J. Chem. Phys.*, **47**, 2921 (1967).

energies as well as a distribution of energy partition which may themselves vary with excitation energy. However, this approach to arriving at ion thermochemistry should not be applied to conventional appearance potential measurements since the latter are not sufficiently precise.

Radical Thermochemistry. Our results may be combined with adiabatic ionization potentials of ethyl and 2-propyl radicals to give heats of formation of these species which may be compared with those obtained from chemical kinetics. A detailed analysis of this type was recently published by Houle and Beauchamp,[8] and we draw on their work for information on radical ionization potentials. In Table VI we compare the heats of formation of ethyl and propyl radicals derived from our ion heats of formation and the radical ionization potentials[8] with those obtained from thermal chemical kinetics.[3,30] The comparison at 0 K removes any additional uncertainty arising from inaccuracy of the ion enthalpy function. It is seen that the isopropyl radical heat of formation agrees within experimental error with the higher of the two values derived from thermal kinetics. However, the value for the ethyl radical is significantly lower.

There are basically three factors to be analyzed, the ion heat of formation, the radical ionization potential, and the kinetics value for the radical heat of formation. As for the last, which lies outside our area of expertise, we note merely that there is compelling evidence that the higher of the two kinetics values is the correct one.[3] Further, we examined the magnitude of the likely error in correcting the high temperature (1100 K) heat of formation of ethyl radical down to 0 K. It was found not to exceed several kilojoules per mole. Thus the problem must lie in the ion measurements. We are faced with seeking to account for ~0.2 eV either in the breakdown curve or in the photoelectron spectrum, whose first significant onset was taken to represent the adiabatic ionization potential. There is no way to devise a plausible source of error of this magnitude and sign which could simultaneously affect all these independent sets of measurements. Thus we conclude, as was done earlier by both Baer[4] and Traeger,[5] that the photoelectron determination is in error. Alternatively, there is a possibility that the fragmentation process does require excess energy which is simply not converted into kinetic energy. The results on primary propyl halides are suggestive, see below.

If the radical ionization potential is in error, the results of the present and previous work would imply that the (0,0) and (1,0) transitions are not observed, i.e., weak. We note that a number of years ago, a photoionization study of the ethyl radical was published,[31] leading to an ionization potential of <8.4 eV, in good agreement with the recent photoelectron study. However, inspection of the published photoionization curves show that there is a weak ion current extending sometimes ~0.1 eV, sometimes 0.2 eV below this 8.4-eV value. A plausible explanation of this is, of course, that this weak current is due to thermal hotbands arising from the pyrolytic method used to generate the ethyl radicals. One could, however, identify this weak photoionization current with the weak Franck–Condon transitions in question. We also note that two electron-impact experiments using the RPD method gave values lower than for the ionization potential,[32,33] although a third measurement employing an electron monochromator did not.[34] The difficulties and limitations of using nonmonoenergetic electron-impact techniques are well-known,[35] but the fact that the measured ionization potentials were indeed lower is unusual and suggestive.

The Proton Affinity Scale. Through determinations of equilibrium constants for proton-transfer reactions

$$AH^+ + B \rightleftharpoons BH^+ + A$$

in the gas phase, there is available now an extensive scale of relative gas phase proton affinities.[1,36] The proton affinity is defined as the enthalpy change of the reaction

$$AH^+ \rightarrow H^+ + A$$

at 298 K. The position of isobutene in the scale has been well established for some time,[1,36,37] and its absolute proton affinity, calculated from available values of $\Delta H_f(t\text{-}C_4H_9^+)$, has often been used as a primary standard for establishing absolute values for the entire proton affinity scale. However, the existence in the literature of several disparate values of $\Delta H_f(t\text{-}C_4H_9)$,[3,38] as well as two values for the ionization potential of this radical,[8,39] has led to some confusion and to wide variations in values ascribed to the proton affinity scale. Other possible primary standards exist, but until very recently, either their position in the proton affinity scale was not well established or the heat of formation of either AH^+ or A was not well-known.

Table VII. The Assignment of Absolute Values (kJ/mol) to the Proton Affinity Scale[o]

M	relative proton affinity[a]	absolute values based on $\Delta H_f(i\text{-}C_3H_7^+)_{298}$ = 798.8 ± 2 kJ/mol	lit values
NH_3	98.3[b]	850.1	860.2[f]
	94.6[c]	846.4	
	93.3[d]	845.1	
$C_6H_5CH_2$	81.2 ± 6.3[e]	833.0 ± 7.9	832.6 ± 5.9[g] 828.9 ± 5.9[h]
$i\text{-}C_4H_8$	54.3 ± 2.1[b-d]	806.1 ± 3.8	816.7 ± 3.3[i] 812.1 ± 5.4[j] 815.5 ± 7.9[k]
CH_3CHCH_2	0.0[d]	751.8 ± 2.9	748.0 ± 2[i] 755.6 ± 8[l] 752.3 ± 4[m]
trans-2-C_4H_8	−0.4 ± 5.0[d]	751.4 ± 6.7	746.8 ± 3[n]

[a] Relative proton affinities from gas-phase basicity scales reported in ref 1, 36, 40, and 41. Temperature corrections discussed in ref 40 are incorporated. Entropy changes were taken as ($NH_3 \rightarrow NH_4^+$), $\Delta S° = -7.5$ J/(deg mol) (includes changes in moments of inertia and rotational symmetry numbers); ($C_6H_5CH_2 \rightarrow C_6H_5CH_3^+$), $\Delta S° = +5.8$ J/(degmol); ($i\text{-}C_4H_8 \rightarrow t\text{-}C_4H_9^+$), $\Delta S° = +2.9$ J/(deg mol) (includes changes in moments of inertia and rotational symmetry numbers and gain of internal rotation with loss of double bond, see ref 37 and 40); ($CH_3CHCH_2 \rightarrow i\text{-}C_3H_7^+$), $\Delta S° \simeq 0$, see ref 40; (*trans*-2-$C_4H_8 \rightarrow$ 2-$C_4H_9^+$), $\Delta S° \simeq 0$. [b] Reference 36a. [c] References 1, 36b, and 36c. [d] Reference 40. [e] Reference 41. [f] Ab initio calculation: R. A. Eades, D. A. Weil, D. A. Dixon, and C. H. Douglas, Jr., *J. Phys. Chem.*, 85, 981 (1981). [g] $\Delta H_f(C_6H_5CH_2) = 203.8 \pm 4.6$ kJ/mol from ref 42a; $\Delta H_f(C_6H_5CH_3^+) = 901.2 \pm 1.3$ kJ/mol from ref 43 and references cited therein. [h] $\Delta H_f(C_6H_5CH_2) = 200.0 \pm 4.6$ kJ/mol from ref 42b; $\Delta H_f(C_6H_5CH_2^+) = 901.2 \pm 1.3$ kJ/mol from ref 43 and references cited therein. [i] Reference 5. [j] Value of $\Delta H_f(t\text{-}C_4H_9^+)$ relative to $\Delta H_f(C_6H_5CH_2^+)$ from Van't Hoff plot for equilibrium: $t\text{-}C_4H_9^+ + C_6H_5CH_2^+ + i\text{-}C_4H_8$ (P. Kebarle, presented at 29th Annual Conference on Mass Spectrometry and Allied Topics, Minneapolis, Minnesota, 1981). $\Delta H_f(C_6H_5CH_2) = 203.8 \pm 4.6$ kJ/mol[42a] and $IP(C_6H_5CH_2) = 7.20$ eV (F. A. Houle and J. L. Beauchamp, *J. Am. Chem. Soc.*, 102, 2540 (1980)). [k] $\Delta H_f(t\text{-}C_4H_9^+) = 696.7$ kJ/mol from $\Delta H_f(t\text{-}C_4H_9) =$ kJ/mol[3] and $IP(t\text{-}C_4H_9) = 6.70$ eV.[8] [l] $\Delta H_f(s\text{-}C_3H_7) = 85.1$ kJ/mol[3] and $IP(s\text{-}C_3H_7) = 7.36$ eV.[8] See Discussion for evaluation of this value. [m] Reference 4. [n] J. C. Traeger, ref 57. [o] All values for heats of formation of neutral molecules used in calculating proton affinity values are from ref 44.

---

(30) S. W. Benson, "Thermochemical Kinetics", 2nd ed., Wiley, New York, 1976.

(31) F. A. Elder, C. F. Giese, B. Steiner, and M. G. Inghram, *J. Chem. Phys.*, **36**, 3292 (1962).

(32) J. M. Williams and W. H. Hamill, *J. Chem. Phys.*, **49**, 4467 (1968).

(33) C. E. Melton and W. H. Hamill, *J. Chem. Phys.*, **41**, 3464 (1964).

(34) F. P. Lossing and G. P. Semeluk, *Can. J. Chem.*, **48**, 955 (1970).

(35) J. H. Beynon, R. G. Cooks, J. R. Jennings, and A. J. Ferrer-Correira, *Int. J. Mass Spectrom. Ion Phys.*, **18**, 87 (1975).

(36) (a) J. F. Wolf, R. H. Staley, I. Koppel, M. Taagepera, R. J. McIver, Jr., J. L. Beauchamp, and R. W. Taft, *J. Am. Chem. Soc.*, **999**, 5417 (1977). (b) R. Yamdagni and P. Kebarle, *ibid.*, **98**, 1320 (1976). (c) Y. K. Lau, Ph.D. thesis, University of Alberta, 1979.

(37) P. Ausloos and S. G. Lias, *J. Am. Chem. Soc.*, **100**, 1954 (1978).

(38) (a) M. Rossi and D. M. Golden, *Int. J. Chem. Kinet.*, **11**, 969 (1979); (b) A. L. Castelhano, P. R. Marriott, and D. R. Griller, *J. Am. Chem. Soc.*, **103**, 4262 (1981).

(39) J. Dyke, N. Jonathan, E. Lee, A. Morris, and M. Winter, *Phys. Scr.*, **16**, 197 (1977).

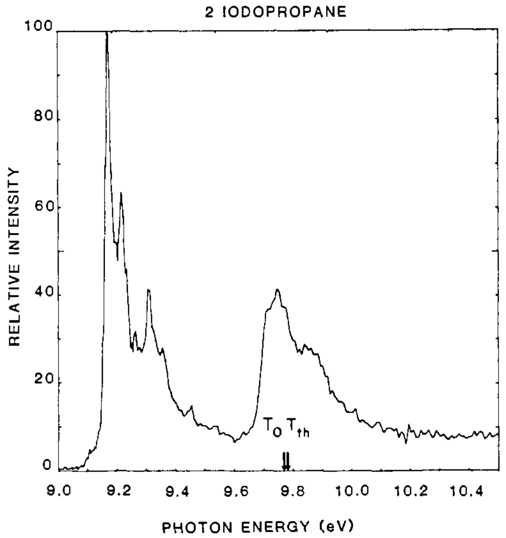

Figure 8. Threshold photoelectron spectrum of 2-iodopropane. The arrows labeled T_0 and T_{th} indicate the energies of the zero-kelvin and thermochemical thresholds, respectively.

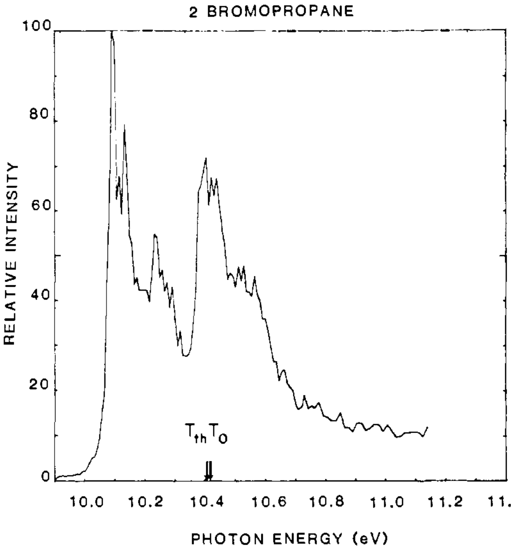

Figure 9. Threshold photoelectron spectrum of 2-bromopropane. The arrows labeled T_0 and T_{th} indicate the energies of the zero-kelvin and thermochemical thresholds, respectively.

Recent work has established the position of propylene in the proton affinity scale.[40] It is of interest to use the value determined here for $\Delta H_f(i\text{-}C_3H_7^+)_{298}$ as the primary standard for the proton affinity scale and to observe how the proton affinities of other possible primary standards agree with those calculated from currently available heats of formation of the relevant ions and neutral molecules. In particular, Traeger and McLoughlin[5] have reevaluated the 298 K heats of formation of several alkyl ions including $t\text{-}C_4H_9^+$. Also, a recent application of a kinetic approach has resulted in an estimation of the position of the benzyl radical in the proton affinity scale;[41] the heats of formation of this radical[42] and its conjugate acid[43] are well-known. An examination of the relationship of these various pieces of data through the proton affinity scale provides a test of internal consistency.

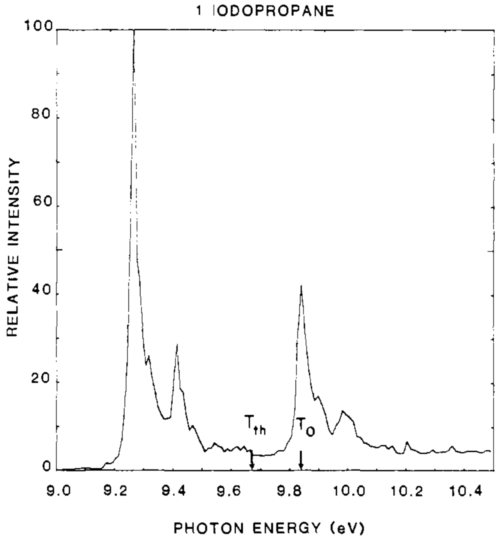

Figure 10. Threshold photoelectron spectrum of 1-iodopropane. The arrows labeled T_0 and T_{th} indicate the energies of the zero-kelvin threshold and the themochemical threshold for formation of the 2-propyl ion.

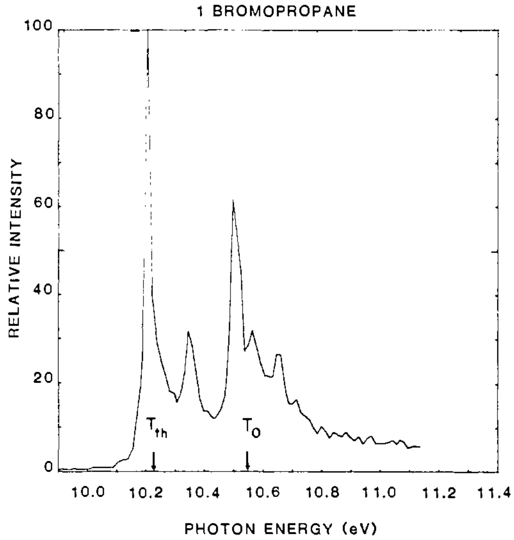

Figure 11. Threshold photoelectron spectrum of 1-bromopropane. The arrows labeled T_0 and T_{th} indicate the energies of the zero-kelvin threshold and the thermochemical threshold for formation of the 2-propyl ion.

The relative proton affinities of propylene, $i\text{-}C_4H_8$, *trans*-2-C_4H_8, and $C_6H_5CH_2$ are given in Table VII. Also shown in the relative value for the proton affinity of NH_3 as determined in several different laboratories. (Ammonia is often cited as a secondary standard for the absolute proton affinity scale in spite of the fact that its position in the scale is not well established.)

A comparison of the absolute values ascribed to the proton affinity scale using CH_3CHCH_2 as base, with proton affinities of $C_6H_5CH_2$, $i\text{-}C_4H_8$, and *trans*-2-C_4H_8 calculated from information in the literature, shows that within the cited error limits, there is now internal consistency among the various possible primary standards for the scale. The proton affinity of propylene derived here appears to be the best established primary standard for the proton affinity scale in that (a) with the exception of the value based on the ionization potential of the propyl radical[8] (discussed above), values for heat of formation of the propyl ion (i.e., the proton affinity of propylene) determined in different laboratories are in agreement, within experimental error and (b) internal consistency of proton affinity values derived from the scale and those predicted by using absolute values for relevant heats

---

(40) S. G. Lias, D. M. Shold, and P. Ausloos, *J. Am. Chem. Soc.*, **102**, 2540 (1980).

(41) M. Meot-Ner (Mautner), submitted for publication in *J. Am. Chem. Soc.*

(42) (a) W. Tsang, *Int. J. Chem. Kinet.*, **10**, 41 (1978); (b) M. Rossi and D. M. Golden, *J. Am. Chem. Soc.*, **101**, 1230 (1979).

(43) S. G. Lias and P. Ausloos, *J. Am. Chem. Soc.*, **100**, 6027 (1978).

(44) J. B. Pedley and J. Rylance, "Sussex-NPL Computer Analysed Thermochemical Data: Organic and Organometallic Compounds", University of Sussex, 1977.

of formation can only be satisfactorily achieved by using this standard.

Fragmentation Mechanism and Kinetics. The mechanism and kinetics of these propyl halides fragmentation processes exhibit a number of interesting features which we will now discuss. The removal of an electron from a nonbonding lone-pair halogen orbital produces a radical cation whose ground state is split into two levels as a result of spin–orbit interaction. Details of this spin–orbit splitting have been discussed by Brogli and Heilbronner.[45] They were able to show theoretically that the splitting is largely independent of the type of alkyl group and that there are conjugative interactions which lead to the vibrational structure observed in the corresponding photoelectron bands.

In Figures 8–11 are shown the threshold photoelectron spectra of the four propyl halide molecules, determined in the present study. The spectra clearly show the spin–orbit splitting, ca. 0.30 eV for the two bromopropanes and ca. 0.55–0.60 eV for the two iodopropanes. The corresponding ionization potentials are in very good agreement with earlier work,[21,45–47] although the intensity ratio of the doublets is not the same in the present threshold photoelectron spectra as in the 58.4-nm spectra. This is due to autoionization effects in the threshold spectra. Also, the threshold spectra show a pronounced vibrational structure, whose origin has been discussed by Brogli and Heilbronner. If now we take the experimental zero-kelvin fragmentation thresholds determined from the breakdown curves, we find that *in all four instances*, these thresholds (T_0) lie just at or slightly above the onset of the upper spin–orbit level. Taking into account the experimental error in the threshold determination and the possibility that the onset of the upper spin–orbit bands of the 2-propyl halides might be lowered by hot band effects, we have the interesting possibility that the fragmentation onset might in all four instances indeed coincide with the adiabatic threshold of the upper spin–orbit state.

As for the thermochemical thresholds, we take the mean value of the 2-propyl ion heat of formation determined from 2-bromopropane and 2-iodopropane and appropriate auxiliary thermochemistry (Table II) and find the following. The thermochemical thresholds for the 2-halopropanes essentially coincide with the experimental thresholds, since they were used to determine $\Delta H_f{}^{\circ}{}_0(2\text{-}C_3H_7{}^+)$. However, on the assumption that the 2-propyl ion would be formed, the thermochemical threshold for this process in 1-bromopropane lies at the ground vibrational level of the ion ground state, and in 1-iodopropane it lies at the upper end of the Franck–Condon envelope of the electronic ground state, see Figures 10 and 11. Thus, with respect to formation of 2-propyl ions the 1-bromopropane certainly and the 1-iodopropane very probably do not fragment even when they possess sufficient energy to do so. The qualified statement for the latter ion arises from our lack of absolute certainty that direct or threshold autoionization is being observed at the thermochemical threshold (see Figure 11). Comparison with the ethyl iodide results suggests that autoionization is taking place, and any reasonable consideration of the Rydberg series leading to the upper spin–orbit limit would suggest this as well. Thus we conclude that a potential barrier exists and has to be surmounted in order to produce the 2-propyl ions from the 1-halopropane precursors. In other words, at threshold primary propyl halides do *not* form primary propyl ions.

The observation of unimolecular metastable transitions in all four halopropane fragmentation processes poses interesting questions about the origin of these comparatively slow fragmentation processes. If the ion fragmented directly from the upper spin–orbit state to form products, one would not expect slow fragmentation in the conventional QET sense since this would correspond to unimolecular decompositions with very small activation energies and rather conventional entropies. Thus one is prompted to ask whether there is prior internal conversion to form vibrationally excited ground-state ions which fragment slowly enough to produce observable metastable transitions.

Table VIII. Fractional Abundance of Detectable Metastable Transitions with Various Decay Rates

$10^6 k$, s^{-1}	$f(C_3H_7I)$	$f(C_3H_7Br)$
0.001	10^{-3}	9×10^{-4}
0.01	10^{-2}	8.7×10^{-3}
0.1	0.08	0.07
0.5	0.16	0.17
1	0.10	0.13
2	0.02	0.04
3	4×10^{-3}	9×10^{-3}
4	10^{-3}	2×10^{-3}
5	10^{-4}	4×10^{-4}
6	1.7×10^{-5}	10^{-4}
7	2.7×10^{-6}	1.9×10^{-5}
time interval, μs	1.83–2.87	1.55–2.44

Table IX. Minimum Fragmentation Rates for Propyl Halide Ions

molecule	I_p, eV	T_0, eV	E_a, eV	$k_{\min}$, s^{-1}
1-C_3H_7I	9.25	9.84	0.59	1.7×10^7
2-C_3H_7I	9.19	9.77	0.58	6.0×10^7
1-C_3H_7Br	10.18	10.55	0.37	6.1×10^8
2-C_3H_7Br	10.12	10.42	0.30	2.2×10^9

The time interval within which a metastable fragmentation process must occur in the double-focusing mass spectrometer can be evaluated from source residence time and trajectory calculations. It is 1.4–2.2 μs for an ion of mass number m/z 100.[16] Thus, depending on the unimolecular decay rate, some fraction of the ions will be detected as metastables. In Table VIII we give the effective time interval and the fraction for various values of the decay rate for the m/z 170 and 123 corresponding to propyl iodide and propyl bromide ions. Referring to this table one can then conclude that for an observed metastable transition to have an abundance relative to the parent of 10^{-4} or more, it must surely arise from an ion population containing a significant fraction with a decay rate less than $\sim 5 \times 10^6$ s^{-1}. Further, a small uncertainty (0.1–0.2 μs) in the absolute magnitude of the effective time interval will not significantly alter this result. The observed fractional abundance of metastable transitions relative to the parent ion is given in Table IV.

One can compare this information with the results of QET calculations. Vestal[48] has shown that the minimum rate at fragmentation threshold is given by

$$k_{\min} = \frac{1}{h\rho(E_a)}$$

where ρ is the reactant density of states and E_a is the activation energy for the process. Using as a first approximation the neutral molecule frequencies as ion frequencies, the minimum rates can be calculated and are given in Table IX. It is seen that the minimum fragmentation rates are faster than those implied by the observation limit of the metastable transitions. The deviation ranges from a factor of 4 for 1-iodopropane to more than 2 orders of magnitude for the two bromopropanes. Before drawing inferences, it is necessary to assess the sensitivity of these numbers to input data.

For small changes in the activation energy, the minimum rates change by 10–20% per 0.01 eV, so that small errors in activation energy do not affect the magnitude of these numbers.

The choice of neutral molecule frequencies to represent ion frequencies is a more delicate matter. Evidently the reactant density of states is sensitive to these frequencies, particularly the low ones. For example, 1-iodopropane (trans conformer) has four torsion and deformation modes with frequencies of 117, 200, 227, and 289 cm^{-1}.[24] The values of these frequencies in the ion are unknown. The molecular orbital treatment of Brogli and Heil-

---

[45] F. Brogli and E. Heilbronner, *Helv. Chim. Acta*, **54**, 1423 (1971).

[46] J. A. Hashmall and E. Heilbronner, *Agnew. Chem.*, **82**, 320 (1970).

[47] R. G. Dromey and J. B. Peel, *J. Mol. Struct.*, **23**, 53 (1974), Figures 1 and 2.

[48] M. L. Vestal in P. Ausloos, Ed., "Fundamental Processes in Radiation Chemistry", Interscience, New York, 1968.

bronner[45] shows that the carbon–halogen bond order of the ion is higher than that of the neutral molecule due to conjugation of the singly occupied halogen orbital with orbitals of the alkyl group. This would produce an increase in some of the force constants. On the other hand, a few vibrational progressions observed in some Rydberg series of primary and secondary alkyl iodides indicate that some frequencies are slightly lower in the Rydberg states.[49,50] Sensitivity studies of the density of states calculations indicate that, if the four lowest torsion and deformation modes are lowered by $\sim$80 cm, the value of $k_{\min}$ is decreased by 1 order of magnitude, reaching a value where 3–5% detectable metastable transitions would occur. It is to be noted that lowering of *all* the frequencies by $\sim$70 cm^{-1} will lead to the same result, illustrating the fact that the low-frequency modes dominate the density of states. It is not inconceivable that these torsion and deformation modes of the ion may be this low.

In the case of 1-bromopropane the lowest frequencies are of the same type and have very similar values 122, 221, 227, and 313 cm^{-1} for the trans conformer.[24] In order to reduce $k_{\min}$ from 6.1×10^8 to about 1.8×10^6, these frequencies had to be lowered by more than 110 cm^{-1} each or, alternately, replaced by a set of values of 30, 40, 50, and 60 cm^{-1} which appears to be entirely unreasonable. The corresponding situation for the 2-iodo- and 2-bromopropanes was similar, leading to even more unreasonable requirements for the frequencies of 2-bromopropane ion.

We are thus faced with a situation where the reactant density of states is apparently not high enough to lead to a minimum rate that is low enough to produce observable metastable peaks. Further, the energy dependence of the rate constant very near threshold is essentially dictated by the integrated number of states of the activated complex and can be estimated to increase by a factor of about 3 within about 0.02 eV. The observed abundance of metastable transitions relative to the parent ion is so high that one is led to attempt the following rationalization of the results. This would be that in all four cases the fragmentation threshold coincides exactly with the ground vibrational level of the upper spin orbit state. Then taking the 58.4-nm photoelectron spectrum as a semiquantitative measure of the energy deposition function for ionization by 70 eV electrons, one would produce a population of ions in that ground vibrational level equal to about 10% of the stable parent ion. This is estimated from the observation that the intensities of the two spin–orbit components are equal, the Franck–Condon transitions are predominantly 0–0, and at room temperature only 10–15% of the molecules are in their ground vibrational level. The crux of the matter is that one has then to assume prior internal conversion into the ground state followed by conventional unimolecular QET decay. And, further, one has to account for the high reactant density of states. In this connection, we have not discussed vibrational anharmonicity because nothing is known for these molecules or ions. We do wish to point out that calculations have been published showing that inclusion of anharmonicity will slightly increase the density of states.[51,52] This is certainly so for cubic or Morse-type potentials in which the level spacing decreases with increasing energy. However, there is also anharmonicity with increasing level spacing, and the torsional and deformation modes in question more likely belong to this class.

One may speculate that the slow fragmentation processes observed here may represent a situation where an essentially vibrationless ion decomposes slowly because of weak coupling of normal modes. Alternatively the slow processes may be due to tunneling which, in principle, could also take place when losing a heavy atom.

The present results, together with earlier studies on bromobenzene[53] and dibromopropane[54] indicate that other halogenated compounds may be found which exhibit slow fragmentation processes. And these slow processes may have other than a conventional QET unimolecular origin.

Acknowledgment. We would like to acknowledge helpful discussions or correspondence with Drs. P. Ausloos, J. C. Traeger, and W. Tsang. M.A.A.F. wishes to acknowledge financial support from the Instituto National de Investigacaō Cientifica, Lisbon, Portugal. J.L.H. thanks the Natural Sciences and Engineering Council of Canada for financial support. Also we gratefully acknowledge the support of this work by the U.S. Department of Energy, Office of Health and Environmental Research, under Contract No. 80EV10373.000.

Registry No. 1-C_3H_7I radical cation, 79240-91-8; 2-C_3H_7I radical cation, 81064-24-6; 1-C_3H_7Br radical cation, 34475-58-6; 2-C_3H_7Br radical cation, 69423-62-7; $C_2H_5^+$, 14936-94-8; *i*-$C_3H_7^+$, 19252-53-0; NH_3, 7664-41-7; $C_6H_5CH_2^{\cdot}$, 2154-56-5; *i*-C_4H_8, 115-11-7; CH_3CHCH_2, 115-07-1; *trans*-2-C_4H_8, 624-64-6; ethyl iodide, 75-03-6; 2-iodopropane, 75-30-9; 2-bromopropane, 75-26-3; 1-iodopropane, 107-08-4; 1-bromopropane, 106-94-5.

---

(49) R. A. Boschi and D. R. Salahub, *Mol. Phys.*, **24**, 289 (1972).

(50) R. A. Boschi and D. R. Salahub, *Mol. Phys.*, **24**, 735 (1972).

(51) Z. Prăsil, L.-K. Huy, and W. Forst, *Adv. Mass Spectrom.*, **6**, 963 (1974).

(52) W. Forst and Z. Prăsil, *J. Chem. Phys.*, **53**, 3065 (1970).

(53) H. M. Rosenstock, R. L. Stockbauer, and A. C. Parr, *J. Chem. Phys.*, **73**, 773 (1980).

(54) J. L. Holmes, F. P. Lossing, and R. McFarlane, presented at the 29th Annual Conference on Mass Spectrometry and Allied Topics, Minneapolis, May 1981.

(55) H. M. Rosenstock in P. Ausloos, Ed., "Kinetics of Ion Molecule Reactions", Plenum Press, New York, 1979, pp 246–249.

(56) D. K. Bohme, G. I. Mackay, *J. Am. Chem. Soc.*, **103**, 2173–2175 (1981).

(57) J. C. Traeger, *Org. Mass Spectrom.*, **16**, 193 (1981).